ce/papers Proceedings in civil engineering

Ernst & Sohn A Wiley Brand

ORIGINAL ARTICLE

eurosteel AMSTERDAM 2023

Ernst & Sohn A Wiley Brand

Fatigue behavior of girder with flange thickness transitions and cope holes - tests and simulations

Stefanie Röscher[1] | Markus Knobloch[1] | Christoph Derler[2] | Martin Langwieser[2] | Harald Unterweger[2]

Correspondence

Stefanie Röscher
Ruhr University Bochum
Faculty of Civil and Environmental Engineering
Chair of Steel, Lightweight and Composite Structures
Universitätsstr. 150
44801 Bochum, Germany
Email: stefanie.roescher@rub.de

[1] Ruhr-University Bochum, Germany
[2] Graz University of Technology, Austria

Abstract

The fatigue behavior of steel girders with flange thickness transition and cope hole has been experimentally analyzed with two large-scale cyclic tests. Special attention is paid to the arising and interacting local effects. The fatigue tests have been conducted in a four-point bending setup. Both girders have shown fatigue-induced failure at the flange butt welds at the thickness transition. The experimental results are presented in terms of fatigue life, differentiating the initiation and propagation life, as well as observed crack position and shape. Moreover, an advanced fatigue life prediction using the Two-Stage-Model is applied to the tested girders. The Two-Stage-Model applies the Strain-Life and the Crack Propagation Approach to assess the total fatigue life. Thereby, the number of cycles as well as the crack shape show a good agreement with the experimental results and proves the applicability of the Two-Stage Model for an advanced fatigue assessment.

Keywords

Fatigue Life, Two-Stage-Model, Thickness Transition, Cope Hole, Cyclic Tests, Strain-Life Approach, Crack Propagation Approach, XFEM

1 Introduction

Flange thickness transitions with cope holes are a common European constructional detail in bridge design. The cross sections of long span girders are adapted to varying bending moments by means of flange thickness transitions to allow efficient design and material use. To simplify assembly and allow non-destructive testing of welds, a cope hole with a radius of typically 40 to 60 mm is made in the web plate at the thickness transition.

The constructional detail "flange thickness transition with cope hole" shows a complex local stress field with local stress concentrations, that significantly influence the fatigue resistance. Details regarding the local load bearing behavior are given in e.g. [1-5]. In summary, the key points can be considered as: (1) the cross-sectional change due to the thickness transition, which results in additional, fatigue-relevant local stresses and stress concentrations in the longitudinal and vertical direction, and (2) a small unsupported part of the flange due to the cope hole, which also leads to additional local stresses. The two local stress fields are close to each other, so that the effects are superimposed on each other as well as on the global stress field. The combined effects decisively affect the fatigue life; however, the effects cannot be accurately determined by classical beam theory.

Experimental studies available in literature investigate either the fatigue life of thickness transitions [1] or of cope holes [4, 6]. So far, there are no comprehensive investigations available on the combined detail including the interaction of the local effects, despite the frequent application in fatigue-prone structures. This paper presents the results of large-scale fatigue tests on girders with thickness transition and cope hole to fill in this research gap. Two welded steel girders made of steel grade S355 J2+N were tested in a cyclic four-point bending test setup. The tests were designed to observe the crack initiation phase and crack propagation phase. The experimental results demonstrate the applicability of advanced local approaches, e.g. Two-Stage-Model considering the Strain-Life and Crack Propagation Approach, for the fatigue assessment of complex constructional details.

2 Crack initiation positions at girders with thickness transition and cope hole

The fatigue-relevant local stress field of the constructional detail "thickness transition with cope hole" comprises the effects of a flange thickness transition and cope hole. A study based on an advanced numerical model reveals the locations with high stress concentrations indicating several potential crack initiation positions as marked in figure 1a with A to D. The study shows that a crack may initiate

https://doi.org/10.1002/cepa.2401

either in the flange plate (positions A, B and C) or in the web plate (position D). This can be explained by the interpretation of the local stress field and is shortly summarized below.

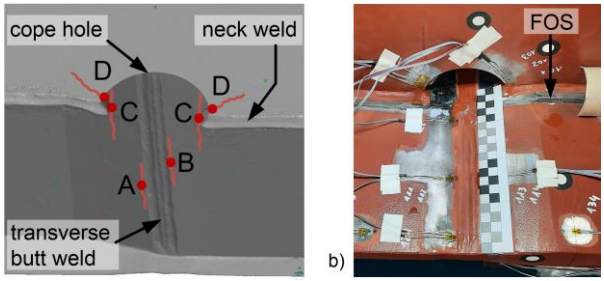

Figure 1 a) Detail thickness transition with cope hole and potential crack initiation positions (A to D), b) applied strain gauges and optical fiber (FOS)

Positions A and B refer to the weld toes of the transverse butt weld in the flange plates. There, the longitudinal normal stresses σ_x define the position for crack initiation at the location with the highest stress concentration. In transverse direction, meaning along the butt weld length, this depends on the combination of the stress distribution in transverse direction, which shows an increase towards the web axis, and the local weld quality, i.e. weld angle, weld toe radius and weld excess, which vary individually over the weld length. Hence, the decisive location along the weld is not clear in advance. Position C marks another potential crack initiation position in the flange plates and refers to the weld toe of the neck weld at the beginning and end of the cope hole. At this position, the longitudinal normal stresses σ_x and vertical stresses σ_z show considerable stress concentrations, affecting the fatigue life. The stress concentration is similar for the beginning and end of the cope in case of pure bending without thickness transition. Though, the stress concentration is altered unevenly when a shear force is present in the girder and a crack will initiate at the side of the cope hole end that faces towards the bearing of a girder [4]. These effects (cope hole, shear force, thickness transition) will be superimposed for the determination of the stress concentration and crack initiation positions.

Another potential crack initiation position lies in the web plate and is marked with D, referring to the second weld toe of the neck weld. At this position, the significant stress concentrations result from the tangential (principal) stresses along the opening of the cope hole. At the end of the cope hole, the stresses are perpendicular to the flange plate and act as vertical stresses σ_z. Here, these local vertical stresses are tensile stresses only, if the thickness transition and cope hole are in a compression flange. Thus, position D marks an often-unattended potential crack initiation position in the global compression flange.

In case of an executed neck fillet weld, the weld root may also serve as a crack initiation position. Though, fillet welds are not desirable within this detail in fatigue-prone structures; this last potential initiation position is listed here for completeness and is not considered in the analysis of the present study.

With the potential crack locations identified, it is not possible to make a general prediction regarding which of the positions of A to D will become decisive for the fatigue design for a girder with thickness transition and cope hole. The determining level of stress concentration is depending on the individual geometry of the detail and girder. Thereby, the transition ratio t_2/t_1 affects the longitudinal stress σ_x as well as the vertical stresses σ_z, although with a different factor. The same applies for the global stress situation, which can consist of pure bending or bending with shear force. The existence of a shear force will generally increase the level of stress concentration, which affects mainly positions C and D. Further, the direction of the thickness transition, meaning increase of thickness either in the direction of the bearing or the midspan, can influence the stress distribution and thus the crack initiation position. This is reflected in the later chosen geometry for the tested girders.

3 Large-scale fatigue tests at girders with thickness transition and cope hole

3.1 Geometry, test setup and test procedure

The geometry of the tested girders, labelled G1 and G2, is given in figure 2. Both girders were 9 m long with a cross section height of 1000 mm and a flange width of 400 mm. Each girder contained four details (D1 to D4) to study, where the flange thickness transition and cope hole were realized. The flange thickness ratio was determined as $t_2/t_1 = 40/20 = 2.0$ with the thinner flange facing midspan. The cope hole radius was R = 50 mm. The investigation details were 2000 mm (2 x h) apart, thus avoiding interaction of the details. The two girders differed only in the design of the neck weld between flange and web plate. Girder G1 showed a neck fillet weld, while girder G2 had a fully penetrated weld in the vicinity of the cope hole. For the chosen geometry, the numerically obtained stress concentrations were in the same range for the potential crack initiation positions A, B and C. This allowed a potential crack initiation at all positions.

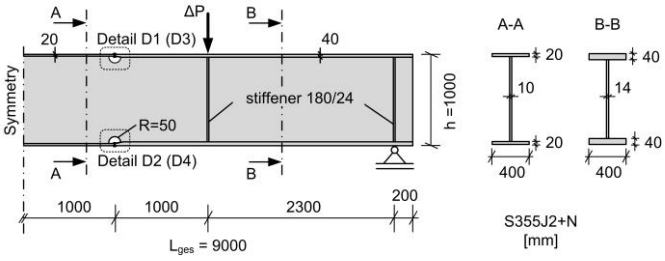

Figure 2 Geometry and static system of the tested girders

For the fatigue tests, the girders were installed horizontally on a sliding plane at the strong floor at the Structural Testing Laboratory of Ruhr-Universität Bochum. The load was applied with two synchronized 1 MN cylinders, as shown in figure 3. In addition to the supports in load direction, a torsional restraint at midspan as well as fork bearings at the supports were realized. The cyclic loading was applied with a nominal stress range of $\Delta S = 175$ N/mm² in the thinner flange plate with a stress ratio of R = 0.1.

For each fatigue test, the test procedure can be divided into two parts. Firstly, the girder was assembled and tested in an initial position as shown in figure 3. Two details (here D1 and D3) were in the tension flange, and details D2 and D4 were in the compressed flange respectively. This led to a first fatigue induced crack at the butt welds in the tension flange, i.e. at detail D1, while there was no detectable damage at the other positions. After reaching a defined final crack length, the girder was reinforced with a bolted lug joint at this crack position, to continue the girder test. Secondly, another crack initiated and grew in the tension flange at detail D3. Again, the crack at detail D3 was observed until the final crack size was reached before the girder was reinforced at this position in the same manner. Secondly, after the successive reinforcement of the first two fatigue cracks in the tension flange, the girder was rotated to a second position, so that tension and compression flanges were replaced. Then, the cyclic test was restarted in the new position to further investigate the fatigue behavior of the remaining two uncracked details D2 and D4 analogously. When referring to the number of cycles within this contribution, only the cycles in tension are stated.

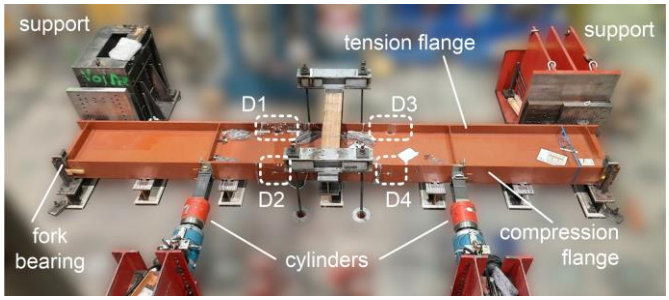

Figure 3 Setup during installation at the strong floor at RUB (top view)

Failure was defined, when the crack reached the outer surface of the flange with a crack length of 40 to 50 mm to still allow reinforcement measures without major deformations in the girder.

3.2 Measurement concept

The fatigue tests were accompanied with a suitable measurement concept to assess crack initiation and propagation at all four details. Strain measurements were conducted using conventional strain gauges as well as two optical fibers (FOS) to assess the stress gradient at the butt weld and DIC-measurements at two investigated details. The various potential crack initiation positions were monitored with carefully positioned strain measurements, as visualized in figure 1b. 3mm linear strain gauges were placed in front of potential crack initiation positions with $0.4t_1$ = 8 mm distance to the weld toe. After crack initiation, the crack depth was measured using a crack depth measurement device based on the alternating current potential drop method (ACPD). Repeated measurements allowed to evaluate the increase of crack depth in combination with the resulting crack shape.

3.3 Material characterization tests

Further, accompanying material characterization tests were carried out. Static properties (E=205700 N/mm², f_y=476 N/mm², f_u=542 N/mm²) were determined using tensile tests; the cyclic parameters (K'=836 N/mm², n'=0.125, σ_f'=813.54 N/mm², ε_f'=0.59, b=-0,77, c=-0.615) were specified by using Incremental Step Tests, and crack growth tests at CT specimens were used to obtain the fracture mechanics parameters for the Paris Law (C=3.22E-13 (N/mm$^{3/2}$)^m, m=2.93). The specimens were obtained from the base material as it is a conservative approach to use the base material characteristics for heat-affected zone and weld material [8]. The explicit consideration of the influence of the weld material or residual stresses was not part of the present study.

3.4 Experimental Results

The cyclic test results are presented in terms of number of cycles for failure describing the total fatigue life N_f. Additionally, a distinction is made between the initiation life N_i and propagation life N_p. Next to the results in terms of fatigue life, the tests are evaluated regarding crack initiation position and crack shape. These results later serve for the validation of a fatigue life prediction using advanced assessment methods.

First, the crack initiation position and crack shape are evaluated. The cyclic loading led to fatigue induced cracks, which occurred in similar manner for both girders. For seven out of eight investigated details, the cracks initiated and grew at the weld toe of the transverse butt welds in the tension flange. The crack was observed every time at the weld toe at the thinner flange plate, as illustrated in figure 4. For one detail (G1_D4) no crack could be observed before the test was stopped due to an unplanned long crack at midspan, which initiated from a tack weld.

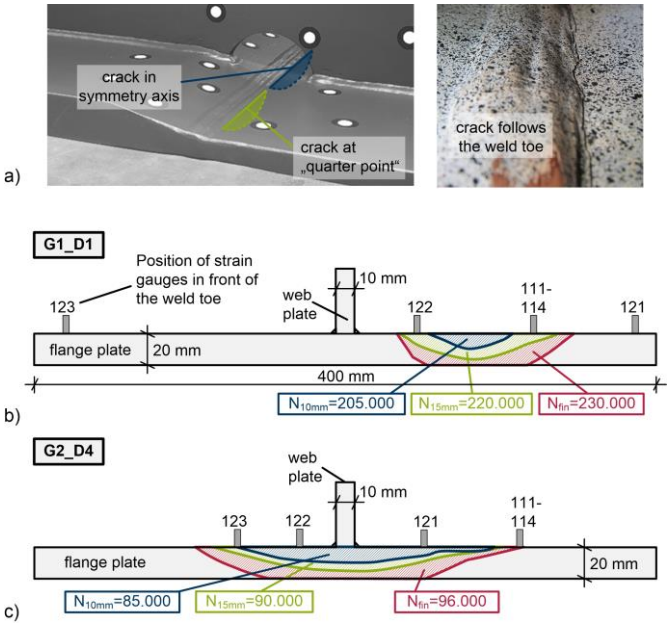

Figure 4 a) Schematic crack position at the transverse butt weld and crack following the weld toe as observed b) typical crack shape at outer flange position c) typical crack shape in symmetry axis

For the seven observed cracks the crack shape was analyzed using the results of crack depth measurements. In each case, an approximate elliptical crack shape could be determined. In comparison, two typical crack shapes could be identified. Either the crack developed approximately at the quarter point of the flange, or approximately in the

symmetry axis of the girder, as presented in figure 4. For all details, the crack growth was observed to increase in depth and length simultaneously. The crack grew in its length parallel to the butt weld along the weld toe and the crack depth increased rectangular in the flange thickness direction. The measured crack shape is illustrated exemplarily for details G1_D1 and G2_D4 in figure 4b and 4c. The colours mark the crack shape at a crack depth of 10 mm (blue) and 15 mm (green) as well as at the end of the test (red), respectively with the corresponding number of cycles in tension.

Next to the crack position and crack shape, figure 5 shows the results in terms of fatigue life for both girders. Within figure 5 the results are given in chronological order. The first four bars refer to girder G1, and the second four bars to girder G2. The hatched bars indicate the results of the second girder position after the rotation, which means these details have already experienced compression cycles. The number of cycles shown here are only the cycles in tension. The detail G1_D4 is marked as run out, as there was no crack growth observed at this position.

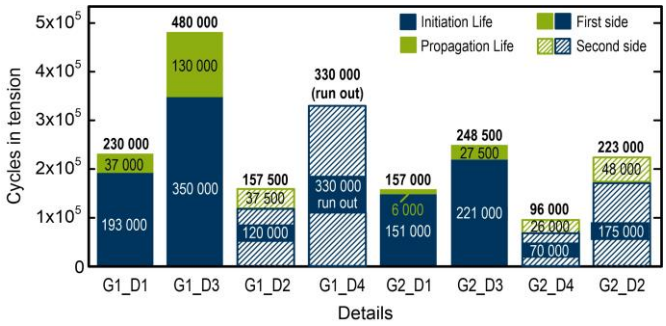

Figure 5 Experimentally determined fatigue life with differentiation of initiation (visually detected) and propagation life (cycles in tension)

The total fatigue life shows a wide range from 96,000 to 480,000 cycles, although the details do not differ in their planned weld execution, weld quality and stress exposure. The comparison of the results shows that there is no marked difference for the results of girder G1 and G2 by differing in the design of the neck weld. Girder G1 reveals overall a slightly higher mean fatigue life than girder G2, but this is within the expected scattering of fatigue tests of welded structures. The notable short fatigue life of detail G2_D1 with only 96,000 cycles allows two interpretations: either the detail inhabited a worse weld quality leading to a reduced fatigue resistance or the preceding cycles in compression led to a damage at the detail that was not detected by means of the applied measurement. Both options will be investigated further.

To verify the test results from this research, comparable fatigue tests from literature are used. In [1] results from a fatigue test of a 5.0 m long girder with a thickness transition ratio of 2.5 and a tapering to the outside are presented. The girder was made of steel grade S235 and tested in a three-point bending test setup with a nominal stress range of $\Delta S = 150$ N/mm² in the thinner flange plate. The fatigue induced crack was observed at the transvers butt weld at the thickness transition, showing a similar type of failure as the present test results in this paper. Both, the results from the present tests (G1 and G2) and from [1] are illustrated in figure 6 within an SN diagram. The loading is given with nominal stress range ΔS in the thinner flange plate.

The experimental results from girder G1 and G2 are given with blue and green markers respectively in figure 6. The results from fatigue tests conducted at TU Graz [1] are given with yellow markers. In summary, the comparison shows a good conformity of the test results indicating that the chosen test setup is appropriate, and the results are reliable; thus suitable to serve as basis for the validation of prediction models.

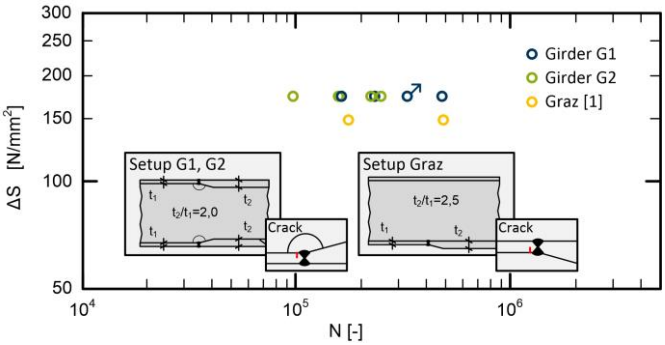

Figure 6 experimentally determined fatigue life (cycles in tension) for the detail thickness transition with cope hole and data from [1]

Next with regard to the total fatigue life, the evaluation of the initiation and propagation phases individually gives valuable information for the following advanced fatigue life prediction.

Regarding the fatigue life prediction using the Two-Stage-Model, the distinction between the number of cycles for the initiation life N_i and the number of cycles for the propagation life N_p is made with the technical crack. The definition for the technical crack differs by various authors. Recently published, the design standard "FKM Richtlinie Nichtlinear" [7] specifies the size of the technical crack with regard to the Strain-Life Approach with 0.25 to 3 mm crack length.

Experimentally, the technical crack can be observed either by visual inspection or with strain measurements. A visual inspection allows to detect only a surface crack. When using strain measurements, a strain increase or decrease serves as indicator for crack initiation, often defined with a change by 5 or 10%. Thereby the time of the change in strain, and thus the definition of the initiation life, depend on the position of the strain gauge with respect to the forming crack. The closer the strain gauge is positioned to the crack, the earlier a change will be registered.

Using a strain criterion for crack initiation for the current investigated detail is complex, because the crack position is unknown in advance. With an unknown crack position, it is not possible to define the position of strain gauges in relation to the forming crack every time alike and will consequently require different threshold values for the change in strain. Nevertheless, the applied strain measurements indicated the forming crack early, so that visual inspection was focused at these positions and therefore the cracks were detected early by visual inspection. It can be concluded that using strain measurements to monitor multiple possible crack initiation positions is applicable. Nevertheless, defining a fixed threshold value of e.g., 5 % strain

increase to determine a uniform and reliable initiation life is not appropriate for this detail due to the varying positioning of strain gauges and cracks. Thus, to distinguish between the number of cycles for the initiation life N_i and the number of cycles for the propagation life N_p for these large-scale girder tests, a visually detected surface crack was used as criterion.

The experimentally determined fatigue life with differentiation of initiation and propagation life is given in figure 5. The initiation life N_i, based on visual detection, is given in blue and the crack propagation life N_p in green. With the chosen differentiation of initiation and propagation lives, the proportion of the initiation life in the total fatigue life is always more than 70%. This is also valid for the details that were exposed to compression cycles in advance. Thus, it can be concluded that the cycles in compression do not cause marked damage at the fatigue-prone butt welds. It is to note that this is based on the evaluation of few details and only for one stress level.

4 Application of the Two-Stage-Model for the fatigue life prediction

A precise fatigue life prediction using the Two-Stage-Model [3, 9] is presented below. The Two-Stage-Model allows SN_f curves to be extracted rather than just predicting the fatigue life for a certain stress range. The evaluation of the SN curves increases the quality of the fatigue life prediction with the possibility to address the low cycle as well as the high cycle fatigue regime.

The fatigue life prediction was carried out for all possible crack positions using the material properties according to section 3.3. It can be summarized, that the initiation life N_i according to the Strain-Life Approach predicts, analogous to the effective notch stress concept, the shortest fatigue life for the weld at the cope hole (position D). Though, when considering the total fatigue life, failure at the butt weld (position B) becomes decisive. Hence, the results presented below are limited to the butt weld. This is in accordance with the test results, while performed fatigue life predictions based on the effective notch stress concept which predicted failure at the web plate, do not coincide with the experimentally obtained results.

4.1 Stage I: Strain-Life Approach

The prediction of the initiation life N_i follows the Strain-Life Approach as presented in [3] for the application to welded structures. The application for the large-scale girders G1 and G2 is summarized shortly. A numerical model for the tested girder geometry was set up in the finite element program Abaqus following the recommendations for the effective notch stress method as given in prEN 1993-1-14 [10] and in DVS0905 [11]. The nominal geometry was implemented with a weld angle of 150° for the butt weld and 45° for fillet welds. Weld toe and weld root were approximated with a fictious notch radius of 1 mm. The quadratic solid elements at the notch had length of 0.18 mm. The model included symmetry and sub models, to achieve a suitable small element size at the notch detail and a larger element size for the global model. Using this numerical model, the geometry can be characterized with the elastic stress concentration factor K_t = 3.4 and the plastic capacity K_p = 3.25 for failure at the butt weld. To assess the damage-relevant hysteresis, the elastic-plastic notch stresses and strains are determined using the Neuber-formula. The successive damage calculation is based on the damage parameter P_{SWT} in combination with nonlinear shape of the P-N curve, based on the strain-life curve of the base material.

The results of the Strain-Life Approach are given as SN_i curve in figure 8 with the dotted line. The curve shows a flat slope. Thus, a change of the elastic stress concentration factor K_t, e.g. due to the local weld geometry, will markedly affect the initiation life. Exemplarily, the change of +/- 10 % in K_t will decrease/increase the initiation life N_i almost by factor 2.

4.2 Stage II: Crack Propagation Approach

To assess the crack propagation phase within this complex detail, a numerical crack propagation calculation is performed following the Crack Propagation Approach. With using XFEM in the crack propagation calculation as presented in [3], the local stress field is reflected and updated continuously for the growing crack shape.

The numerical model was slightly adapted regarding the element size. The initial crack is implemented with a size of a = 0.5 mm crack depth and a corresponding crack length of c = 2 mm. With a given initial crack, the crack growth followed the Paris-Law. The crack shape evolved according to the solution dependent stress distribution. Failure for the numerical approach has been considered analogously to the fatigue tests with a crack length of 40 to 50 mm at the outer side of the flange, unless the limiting threshold value of fracture toughness has been reached beforehand.

The results of the Crack Propagation Approach are given as SN_p curve for the butt weld in figure 8 with the dashed line. Another result of the numerical crack propagation calculation is the resulting, non-predefined crack shape as shown in figure 7. The numerically obtained crack shapes are shown exemplarily for the crack initiation in the web-axis and quarter point of the butt weld, respectively. Only small differences occur, when comparing the experimentally and numerically obtained crack shapes. The numerical crack shape does not follow the weld toe as strict as the experimental results. Further investigations will indicate whether this results from the numerically implemented fictitious notch radius, the material notch effect or the considered mixed-mode-behavior. Nevertheless, the good accordance of experimentally and numerically obtained cracks shows that the approach is capable of reproducing the crack shape with sufficient accuracy even for a complex geometry.

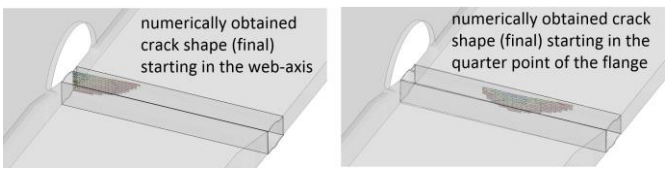

Figure 7 numerically obtained crack shape at the transverse butt weld using XFEM

4.3 Total fatigue life and comparison to test results

The total fatigue life N_f is determined from the individual results of stage I and II as given in sections 4.1 and 4.2. Figure 8 shows the SN_i, SN_p and SN_f curves for failure at the butt weld. The obtained SN_f curve for the total fatigue life is given with the blue curve. The curve shows a flat slope, especially for low stress ranges, which means consequently that small changes in input parameters, such as material properties or local weld geometry, result in major changes in the fatigue life. As expected, the initiation life governs the high cycle fatigue regime, while the propagation life governs the regime with high stress ranges.

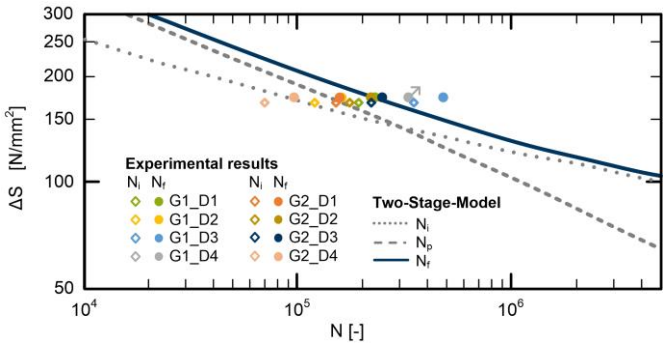

Figure 8 SN_i, SN_p and SN_f curves for the butt weld and experimental results from G1 and G2. In order to make all marks recognizable, the unfilled diamonds are visualized with an offset downwards.

Next to the predicted SN curves, the experimental results from girders G1 and G2 are given in figure 8 as well. In detail, the experimental results are given with their initiation life N_i marked with unfilled diamonds and with the total fatigue life N_f marked with filled circles. Thereby, it becomes clear, that neglecting one of both phases in the design would lead to a conservative fatigue life prediction. The results coincide well with the obtained fatigue life prediction.

5 Conclusion

Two large-scale girders have been successfully tested to analyze the fatigue behavior of the detail "thickness transition with cope hole". Thereby, crack initiation and following crack growth have been observed similarly for all investigated details with a fatigue induced crack at the weld toe of the butt weld at the flange thickness transition. There were no cracks observed at the cope hole in the web plate.

For the studied complex constructional detail, the Two-Stage-Model indicates the correct failure position and crack shape. Thereby, the existing geometry has a high sensitivity of prediction with respect to the input parameters in determining the fatigue life. The application of the Two-Stage-Model leads to a reliable prognosis of the fatigue life.

6 Acknowledgements

This work has been carried out as part of the DASt research project No. 21739 N, financed by the German Federation of Industrial Research Associations' Otto von Guericke' e.V. (AiF). Further thanks are given to the companies Haslinger Stahlbau and MCE for fabrication of the tested girders.

References

[1] Taras, A.; Unterweger, H. (2013) *Proposal for a stress modification factor for the fatigue design of flange thickness transitions in welded girders*. Engineering Structures 56, pp. 1758–1774.

[2] Derler, C.; Unterweger, H.; Knobloch, M.; Röscher, S. (2023) *Fatigue behavior at flange thickness transition with cope hole - design model for engineering practice*. Submitted for Eurosteel 2023.

[3] Röscher, S.; Knobloch, M. (2021) *Fatigue Life Prediction of Welded Girders with Flange Thickness Transitions and Cope Hole*. ce/papers 4, pp. 1172–1182, doi: 10.1002/cepa.1410.

[4] Miki, C.; Tateishi, K. (1997) *Fatigue strength of cope hole details in steel bridges*. International Journal of Fatigue 19, 6, pp. 445–455.

[5] Haghani, R.; Al-Emrani, M.; Heshmati, M. (2012) *Fatigue-Prone Details in Steel Bridges*. Buildings 2, 4, pp. 456–476, doi: 10.3390/buildings2040456.

[6] Stallmeyer, J. E.; Munse, W. H.; Goodal, B. J. (1957) *Behaviour of welded built-up beams under repeated loads*. Reprinted from Welding Journal, Urbana, Illinois.

[7] Fiedler, M.; et al. (2019) *Richtlinie Nichtlinear. Rechnerischer Festigkeitsnachweis unter expliziter Erfassung nichtlinearen Werkstoffverformungsverhaltens für Bauteile aus Stahl, Stahlguss und Aluminiumknetlegierungen*. FKM-Richtlinie. VDMA Verlag GmbH. Frankfurt am Main.

[8] Bissing, H.; Knobloch, M.; Rauch, M. (2023) *Prognosemodelle zur Lebensdauer und zum Weiterbetrieb von Windenergieanlagen – P1398.* Fosta, Düsseldorf.

[9] Röscher, S.; Knobloch, M. (2019) *Towards a prognosis of fatigue life using a Two-Stage-Model*. Steel Construction 12, 3, pp. 198–208.

[10] prEN 1993-1-14 (2022) *Eurocode 3: Design of steel structures - Part 1-14: Design assisted by finite element analysis*, Final Document for CEN Enquiry, CEN/TC250/SC3 N3453.

[11] DVS Merkblatt 0905 (2021) *Industrielle Anwendung des Kerbspannungskonzeptes für den Ermüdungsfestigkeitsnachweis von Schweißverbindungen*. DVS Verband, Düsseldorf.